Fahmy *et al. Heritage Science (2022)* 10:61
https://doi.org/10.1186/s40494-022-00699-1

Heritage Science

RESEARCH ARTICLE

Open Access

Geoenvironmental investigation of Sahure's pyramid, Abusir archeological site, Giza, Egypt

Abdelrhman Fahmy[1*], Eduardo Molina-Piernas[1], Salvador Domínguez-Bella[1], Javier Martínez-López[1] and Fatma Helmi[2]

Abstract

Abusir is the name of an elaborate burial area in Egypt, dotted with 19 pyramids and other temples, stretching on the western side of the Nile from the south of the Giza Plateau to the northern rim of Saqqara. It seems to have been created as the resting site for the Pharaohs dated from 2494 to 2345 BC. The name Abusir, originally spoken as Busiri, means "Temple of Osiris". Over time, the name has become so popular because more than 60 villages now carry this name, but only one is the archaeological site. This paper focused on one of its most important pyramids from the Abusir archaeological area, Sahure's pyramid, since it is one of Egypt's little-known but heavily damaged treasures. Field and laboratory studies have been carried out to investigate and understand the durability problems and construction materials of this pyramid, leading to results that confirmed the impact of the geoenvironmental conditions on the pyramid's architectural, structural, and engineering stability. Moreover, the results showed that mineralogical content in the construction materials was an intrinsic problem due to the presence of swellable (expansive) clays, which are considered responsible for pyramid decay and damage. In addition to external factors such as the effect of temperature variations, rain, pollutants, wind, and earthquakes and their interactions with intrinsic building material defects. Finally, this paper revealed a new discovery for basaltic mortar as the first trial for green concrete manufacturing in the Egyptian Old Kingdom, Fifth Dynasty.

Keywords: Abusir archaeological site, Sahure's pyramid, Geoenvironmental factors, Petrological characterization, Petrophysical properties, Geochemistry, Stone decay, Sandy limestone, Mortar

Introduction

Studies on the impact of geoenvironmental conditions and how external agents affect construction materials are a recurring topic in new construction but are especially important in the materials of historical and archaeological heritage since its understanding will allow better preservation of this cultural heritage [1]. There are several previous studies on stone weathering; for example, Charola et al. [2] explained salt weathering for porous building materials and showed some related deterioration patterns on archaeological stone masonry because of environmental conditions such as fissures, granular disintegration, splitting in building materials, and salt efflorescence. Fitzner and Heinrichs [3] presented a study about weathering impacts on monumental stones and their forms and rates. In addition, they showed the nonvisible/nanoscale deterioration patterns of archaeological stones, visible deterioration in micro- and meso/macroscale-like mass loss, and structural stability. Grossi et al. [4] studied the effect of air pollution, salt weathering, and climate change on the durability of archaeological stones, showing that the blackening of the stones returned to high levels of sulfate deposition, diesel soot, and nitrogen deposition from vehicular sources around the archaeological buildings. Additionally, Figueiredo et al. [5] studied the degradation factors that affected

*Correspondence: abdelrhman.fahmy@uca.es; abdelrhmanmuhammedfahmy@gmail.com

[1] Department of Earth Sciences, Faculty of Sciences, University of Cadiz, Campus Río San Pedro, 11510 Puerto Real, Spain
Full list of author information is available at the end of the article

some Roman archaeological buildings due to the effect of lichen exudates that led to observed physical and chemical alterations in granite. Sandrolini et al. [6] studied the environmental aggressiveness on historical stonework and the weathering patterns and rates using the material identification method and structural finite element modelling to identify the decay causes and outline the efficient restoration procedures. Khanlari et al. [7] showed the influence of freeze–thaw cycles on the mechanical and physical properties of archaeological sandstone and concluded that the pore size distribution plays an essential role in the resistance of sandstones during freeze–thaw cycles. Derluyn et al. [8] explained the damage of salt weathering on building materials and compared the damage of thenardite and halite salts. Additionally, they used high-resolution neutron radiography simultaneously to monitor the crystallization process and deformations. Their results showed that cracking occurred during the drying for the limestone samples due to halite, and no damage was observed during drying due to thenardite. Hemeda [9] explained and studied the climate change risks on archaeological sites in Alexandria and their impacts on building materials and concluded that. In addition, Risdonne et al. [10] used analytical techniques to identify plaster surfaces and evaluate weathering byproducts. Moreover, Villacreses et al. [11] interpreted the impacts of environmental conditions on the mechanical stability and behavior of masonries, especially earth walls. Finally, Hatır et al. [12] determined very specific deterioration maps to identify and qualify the weathering forms in the archaeological sites.

Specifically, in Egypt, several studies have been carried out to study the effect of environmental conditions and climate changes on archaeological sites. For instance, in the Giza pyramid area, Emery [13] studied the weathering conditions on the Great Pyramid and revealed four types of limestone used to build it, such as gray hard dense limestone, soft gray limestone, gray shaly limestone, and yellow limy shaly sandstone. Furthermore, Hanafy and Holail [14] presented a diagnosis study of the middle Eocene "nummulite bank" of the Giza Pyramid Plateau and explained that the early diagenetic alteration of the rock matrix was followed by partial to complete dolomitization of the limestone matrix and nummulite grain. Reader [15] studied the weathering problems and erosion on Sphinx and presented a geomorphological study for Giza Necropolis. USAID of Egypt [16] presented an assessment report to study the environmental impacts on the Giza plateau and suggested a methodology for groundwater lowering. In addition, Gandah [17] studied and discussed the environmental impacts of rain, wind, and salts on the pyramid of Khufu and presented hypotheses for restoration and conservation. Zalewski [18] studied and gave us the opportunity to see the construction materials of the Great pyramid in his study through the petrography observations of the building stones. Finally, Hemeda and Sombol [19] studied and discussed the durability problems of the Great pyramids and the effect of subsurface and underground water on the stability of the pyramid.

In Saqqara necropolis, Madkour and Khallaf [20] explained the degrading process of the faience inside the step pyramid, and the results showed that salt crystallization from the wall support (Bedrock) was the main problem that generally affected the faience and the substructure of the pyramid. Kukela [21] studied the degradation patterns for the Step pyramid of Saqqara and showed isometric deterioration maps for the pyramid. Furthermore, Khalil et al. [22] showed the effects of strong ground shaking on the stability of the Step pyramid and showed that there are many earthquakes in Greater Cairo with low magnitudes but with accumulative effects for the long term on the pyramid. Additionally, Rossi [23] utilized the advanced digital documentation method to monitor the area of the New Kingdom in Saqqara and showed the effect of wind, humidity, and temperature on the archaeological building. Finally, Ahmed [24] described the deterioration patterns for all faces of the Step pyramid and showed the geoenvironmental challenges, such as earthquakes, over the Step pyramid. In Dahshour necropolis, Hemeda et al. [25] studied the geoenvironmental impacts and structural problems on the northern pyramid of Snefru at the archaeological site. Often, there are no more studies that investigate the geoenvironmental problems and material characterizations at the Dahshour and Abusir archaeological sites. Accordingly, the present study is a significant study to investigate the durability and environmental problems of the construction materials of Sahure's pyramid at the Abusir archaeological site.

Of the sixty villages named Abusir in Egypt, only one is an archaeological site of first-class importance. It is located in the southern direction of the Giza Plateau and north of the Saqqara archaeological site and is considered one of the most enriched archaeological sites of the Memphis necropolis [26]. The ancient name of Abusir is called Busiri "the house or temple of the Osiris". It has a cemetery of the Fifth Dynasty kings, but its actual history is much older than the Fifth Dynasty because in the Early Dynastic Period (c. 3150-c. 2613 BCE), it became a rapidly growing cemetery. In the south, close to the Early Dynastic cemetery in northern Saqqara, a rich upper-middle-class cemetery dating from the First and Second Dynasties was discovered at the beginning of the twentieth century by a German archaeological expedition directed by Hans Bonnet [27]. At the beginning of the

1960s, two Italian scholars, Vito Maragioglio and Celeste Rinaldi, contributed to the research on Abusir to make a survey for the site and provided us with rich information on the Abusir pyramids and development plans of the monuments [28]. At the same time, a Czech archaeological expedition started to work in this area, and in the mid-1970s, the Czech team transferred its research to the not yet investigated southern area of the necropolis, and this institute is carrying out excavations at Abusir until now led by Miroslav Bárta [29]. Abusir was the only short-lived cemetery with pyramid complexes of three kings of the Fifth Dynasty: (1) Sahure; (2) NeferirKare; and (3) Niuserre [30] (Fig. 1a and b). In 2015, Abusir was scanned and modelled by the Czech Institute of Egyptology and the Japanese team to document the NeferirKare pyramid with a 3D scanning laser and gave us 3D images for the pyramid to provide both qualitative and quantitative information for the pyramid and its preservation state [31].

Abusir is a sophisticated archaeological site with different kinds of building materials and pyramids. The preservation state of this site is extremely poor and forgotten. Sahure's pyramid has been affected by damage from various geoenvironmental impacts. In this sense,

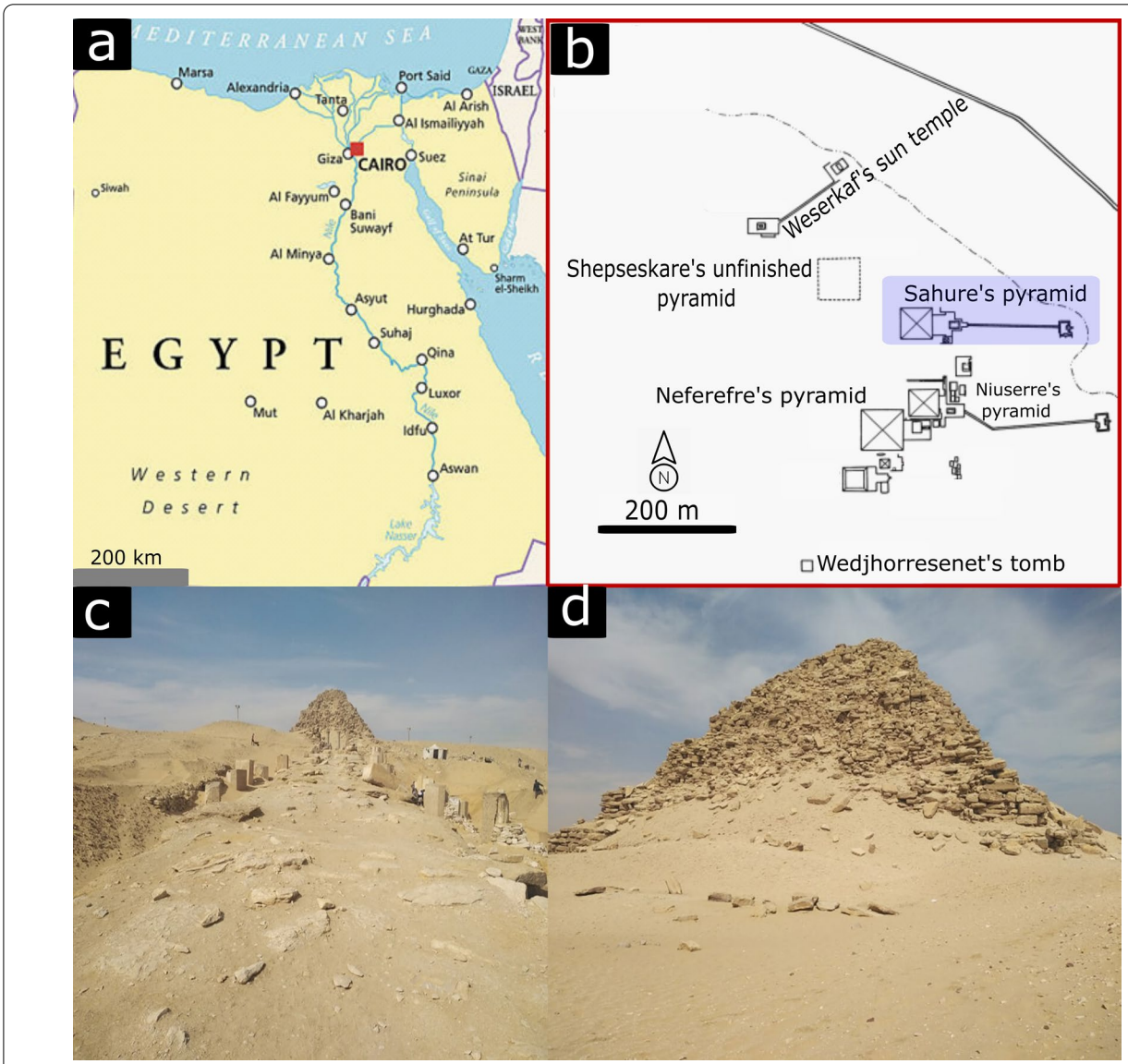

Fig. 1 **a** General map of Egypt and location of the Abusir archaeological site in Giza. **b** Pyramids at the Abusir archaeological site and specifically the Sahure's pyramid (edited after http://www.narmer.pl/map/abusir_en.htm). **c** General view of Sahure's pyramid from the causeway of the pyramid. **d** The preservation state of the pyramid

the durability and resistance of the pyramid decreased physically and mechanically (Fig. 1c and d). For all these motives, the main aims of this paper are (1) to identify the geological and meteorological conditions related to this site; (2) to characterize the construction materials of Sahure's pyramid by means of geochemical, petrographical, and petrophysical approaches; (3) to evaluate the durability and vulnerability of the ancient construction materials of the pyramid; and (4) to present a proposal for scientific conservation and protection of the pyramid. To achieve all these aims, this study has carried out a hazard analysis for the construction materials of the pyramid utilizing different analytical and examination techniques of X-ray diffraction, X-ray fluorescence, and optical microscopy. In addition, the physical properties of the core building material of the pyramid are determined to confirm the environmental impacts on the physical properties of the construction materials used.

Sahure's pyramid context

Description of Sahure's pyramid

Sahure's pyramid is located on a hill, and the elevation from the valley temple adjacent to the Nile is approximately 20 m. It is relatively small because it has a base of approximately seventy-eight meters and rises to a height of forty-seven meters (Fig. 2a and b). According to Verner [32], this pyramid was built using better quality stone and more diverse types than the pyramids of the Fourth Dynasty. For example, the base presents at least two layers of limestone, but it has not been excavated until now. Additionally, the core of the pyramid was composed of six steps of limestone jointed with mud mortar, and the entrance located to the north was cased in fine white limestone from Massara (Fig. 2a). On the other hand, casing stone was built from massive limestone blocks with dimensions of $5 \times 5.5 \times 1$ m, which were prepared and brought from the Tura and Massara quarries [33]. The same materials and quarries were the sources of the casing stones at Neferefre's (unfinished pyramid) and the Great Pyramid [32]. Meanwhile, the inner chambers of Sahure's pyramid were cased by using smaller blocks [33]. The core of the pyramid was packed with a rubble fill of limestone chips, pottery shards, sand, and clay mortaring [32–34]. This construction technique was performed to reduce the cost, effort, and time for pyramid construction. Additionally, the architects made a notable error in planning the base, causing the southeast corner of the pyramid to extend 1.58 m to the east [32] (Fig. 2b).

Architecturally, the pyramid is surrounded by limestone, which is used for paving, but the mortuary temple is paved by basalt and is accessed from the temple's north and south sides with a tall courtyard and rounded enclosure wall 3.15 m thick [35]. On the other hand, the pyramid substructure access is found slightly above ground on the pyramid's north face [32]. A short descending corridor lined with granite leads into a vestibule [34]. In addition, the route and its walls are cased and guarded by a pink granite portcullis (Fig. 2a) [32, 36]. The descending corridor is 4.25 m long with a slope of 24°48′ and has a passage 1.27 m wide and 1.87 m high [34, 37]. The corridor following is lined with limestone begins with a slight ascent before becoming horizontal land lined with granite [34]. The ascending portion is 22.3 m long with a slope of 5°, while the horizontal section is 3.1 m long [37]. Finally, the burial chamber is a single chamber measured to be 12.6 m east–west and 3.15 m north–south [32, 34, 36].

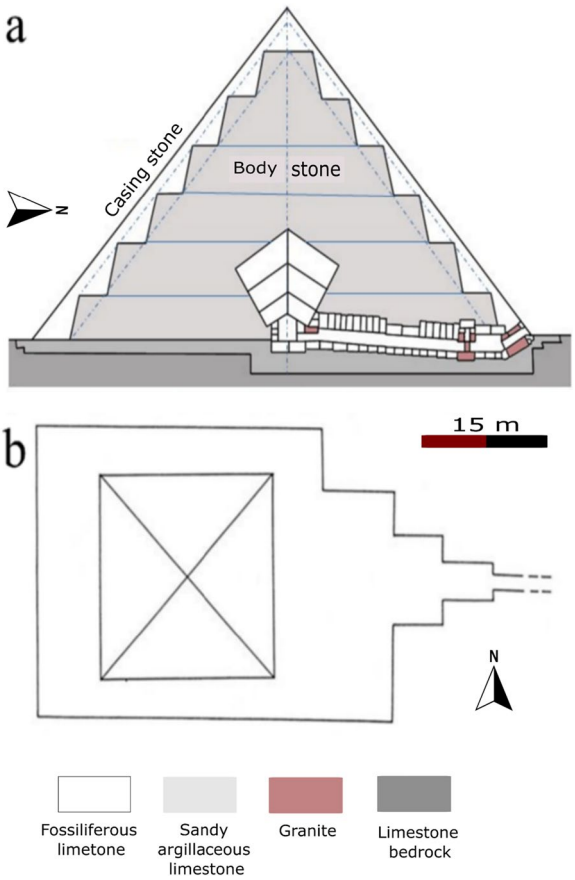

Fig. 2 **a** Cross section and **b** Plan of the Sahure pyramid. The colors in cross-section represent the white fossiliferous limestone from the Tura quarry (casing stone, in white); the body of the pyramid made by laminated sandy argillaceous limestone (marl, in white gray); granite (casing for entrance and some parts in the corridor, in red); and bedrock from limestone (in dark gray). Edited after Ref. [35]

Geological context

Generally, the Memphis area consists of different geological features, such as Nile silts, which are located on the

eastern and western sides of the Nile River and adjacent to the archaeological sites in Memphis, Wadi (Valley). In addition, deposits include neonile deposits, pronile deposits, undifferentiated pronile deposits, limestone intercalated with shale stones, and Cretaceous formations [38] (Fig. 3a). Specifically, Abusir geological formations are considered from the Late Eocene, and Maadi limestone, clay-limestone, and marls crop out (tafla) (Fig. 3a and b). The upper member of the Maadi Formation (blue legend, Fig. 3b), which is connected to the Abusir area, is developed mostly as porous brown sandy limestone in-tempestite facies [38]. According to Bebermeier et al. [39], ancient settlements are covered by more than 7 m of alluvial and aeolian deposits. These formations of Mokattam (Qn2, Fig. 3b) and Maadi are repeatedly intercalated with fossils such as oysters, nummulites, and shale or sandy shale. Moreover, Bebermeier et al. [39] said that the fluvial sediments belonging to a former river system called prenile deposits (Qns, Fig. 3b) occupied the present-day Nile basin in the early Pleistocene. In the middle Pleistocene, the prenile deposited fluvial sediments (Qn2, Fig. 3b) east of the (Qns) deposits, closer to the present-day floodplain of the river Nile. These sediments (Qns and Qn2) were deposited directly on top of Eocene bedrock. Sahure's pyramid is located on the Nile silts (Qns), which reflects the geotechnical problems of the pyramid from the beginning of the construction due to the clay to claystone base (Fig. 3b).

Stone quarries and pyramids construction materials

Generally, ancient Egyptians exploited approximately 200 quarries (Fig. 4) as sources of different kinds of stones, which were used as architectural, ornamental, and structural elements to build their temples, tombs, and pyramids from the predynastic era to the late Roman period, but limestone and sandstone were the dominant building materials for their buildings [40, 41]. In fact, most of the limestone blocks used by ancient Egyptians were brought from Tertiary formations, mainly Eocene, Paleocene, and Pliocene. In addition, some limestone building materials were from the Quaternary age. On the other hand, most of the sandstone blocks were prepared from Cretaceous Nubian formations [40–42]. Specifically, the stones and joint materials (mortars) of the pyramids are important and interesting to reveal much information related to ancient technology and their sustainability [25]. Pyramids were built from different kinds of stones, such as limestone, sandstone, sandy limestone, basalt, and granite. Cutting and preparation of stones from different quarries were an important process as the primary step for preparations of blocks of pyramids using different kinds of tools and techniques, such as using dolerite and crushed quartzite with sands in polishing of the stone surfaces [43] (Fig. 4).

Ancient Egyptian architects depended on different kinds of stones based on their quality, and they exploited dozens of quarries to extract different materials (Fig. 4, gray squares). For that, they used high-quality limestone in the pyramid's casing and its internal chambers [44]. Additionally, they used granite in the casing of the internal chambers, corridors, and bases. In addition, they used basalt in the pavements for mortuary temples for the pyramids, which represents approximately 20% of the pyramid construction. On the other hand, the remaining 80% approximately corresponds to the core part of the pyramids and was brought from local quarries, such as those placed in the Giza Plateau, Abusir, Saqqara, and Dahshour [25, 44, 45]. Tura and Massara quarries (Fig. 4, red circle) were the main places to extract high-quality limestone types that had been used as casing stones for the pyramids and their elements. In addition to the tombs and temples. Both quarries are located near Cairo on the eastern bank of the Nile from pyramids [46]. The Widan El-Faras quarry (Fig. 4, yellow circle), in the northern Fayoum, was the source of the basalt stones for the pavements of mortuary temples from the Old Kingdom. This stone was used on the floor of the mortuary temple of the pyramid with a height of 0.4 m, width of 25 m, and length of 15 m [47]. The local quarry of Abusir and the surrounding area was the source of the core building material of Sahure's pyramid that is adjacent to the local quarry of Saqqara and Dahshour archaeological site as sources of their pyramid core stones (Fig. 4, blue circle). Additionally, to reduce the huge mining work to extract the stone blocks from the local quarry, they used the geomorphological structures and beds to be part of Sahure's pyramid, such as the causeway that connects the valley temple and mortuary temple of the pyramid [39].

Geoenvironmental context

Egypt is a country susceptible to climate change and geoenvironmental hazards such as sea-level rise, in addition to an increase in the intensity and frequency of temperature, wind (with sand and dust storms), heavy rains, and flash floods [48, 49]. Many geoenvironmental conditions affect the area of Abusir, especially temperature fluctuations, strong winds, and humidity. These environmental factors lead to physiochemical and mechanical damage to the structural materials and result in partial or total decay and collapse in some parts of the pyramids.

Recent analyses of the current climatic tendency reveal a warming trend in recent decades in Egypt, with average temperature increases of 1.4 °C and 2.5 °C projected by 2050 and 2100, respectively [50]. In this sense, climate change has been notable for the last ten years and has

had a risky impact on archaeological building materials, such as the thermal stress effect that leads to accelerated decay in stone construction materials. Moreover, the variation in temperature causes changes in material volume, especially when material deformations occur heterogeneously, which leads to differential strains in the stone body [51].

From the readings and recordings for meteorological data in Giza, meteorological Station ID: EGE00147729, it is noticed that the warmest month of the year is July, with an average temperature of 27.5 °C and an average annual temperature of 14.5 °C. On the other hand, the driest month is May with 0 mm, and the wettest month is January (4 mm) (https://en.climate-data.org). Moreover, rainfall is considered rare, with an annual average of 12 mm. However, rainwater, as concentrated in the northern part of the country, is between 150 and 200 mm and decreases gradually to the south, reaching approximately 24 mm. Meanwhile, rainfall on the Mediterranean coastal strip decreases eastward from 200 mm/year at Alexandria to 75 mm/year at Port Said. It also declines inland to approximately 25 mm/year near Cairo and 1 mm/year at Aswan. Moreover, significant intensities of rainfall are recorded on parts of the Red Sea coast. In addition, humidity ranges between 70 and 72% in the northern part of Egypt during the summer months and reaches 13% in the southern part of the Nile valley at Aswan [52].

Additionally, Egypt experiences dust storms in spring and early summer, with dry and windstorms usually arriving in April but occasionally occurring in March and May. The winds flow in low-pressure areas in the Isthmus of Suez and sweep across the northern coast of Africa, reaching high velocities. In addition, they carry large quantities of sand and dust from deserts that extend strongly from the red sea and Nile River to the Mediterranean Sea and from the north-northeast to south-southwest with large amounts of sand and dust (Fig. 5a–d). These sandstorms, often accompanied by winds of up to 140 km, can cause temperatures to rise as much as 20 °C in two hours and may blow continuously for three or four days at a time, followed by an inflow of much cooler air [53].

Air pollution is considered one of the environmental factors and challenges that affects the stones of Sahure's pyramid because it causes chemical weathering of the construction materials and thick black crust over the stone surfaces [54]. In Giza, it is noticed that from September to November, the number of pollutants decreases. On the other hand, in the season of wind, when the sky is strongly dark and strongly dark from March to May, the amount of pollutants increases, such as carbon monoxide, nitrogen oxides, ozone, and sulfur dioxide [55].

Intrinsic factors

Intrinsic factors are defined as the internal problems of the construction materials, which are related to the chemical, physical and mechanical properties of the stones, and intrinsic problems are also related to the interaction between the environmental conditions and the intrinsic properties of the pyramid construction materials. Both intrinsic agents and geoenvironmental agents work together in pyramid stone decay. For example, gypsum salt is detected by means of chemical analysis in the weathered casing limestone of the pyramid due to the reaction between sulfate pollutants and carbonate to produce gypsum [56]. In this sense, and from in situ visual and macroscopic examinations, it is noticed that the fabric of stone is full of impurities and stained areas with yellowish spots, which reflects the weakness of the construction materials of the pyramid.

The main composition of the pyramid construction is yellowish sandy limestone as a core building material and white limestone as casing building material. Therefore, calcite is a common mineral in construction materials and is always exposed to variable and severe environmental conditions, such as humidity, pollutants, and heavy rains; accordingly, calcite is dissolved in water and reacts with outdoor pollutants [57]. Additionally, the decay of the pyramid stones occurred due to the incompatibility in physical and mechanical properties between the casing and core stones, especially during their differential reaction with environmental conditions [57]. Core stones were quarried from the Abusir local quarry, and the natural beds are characterized by high porosity and inhomogeneity. On the other hand, the casing stones are characterized by very low porosity and homogeneity [44], which reflects the extent of the difference in the physical properties between these two kinds of construction stones. Therefore, the environmental interactions will

(See figure on next page.)

Fig. 3 **a** General geological map of the Memphis area and **b** a simplified geological map of the Abusir area. As shown in the legend, the pyramid is connected to the Mokattam formation and Maddi formation. Sahure's pyramid is located on Nile deposits/silt that was deposited directly to cover the Eocene bedrock. Edited after Ref. [39]

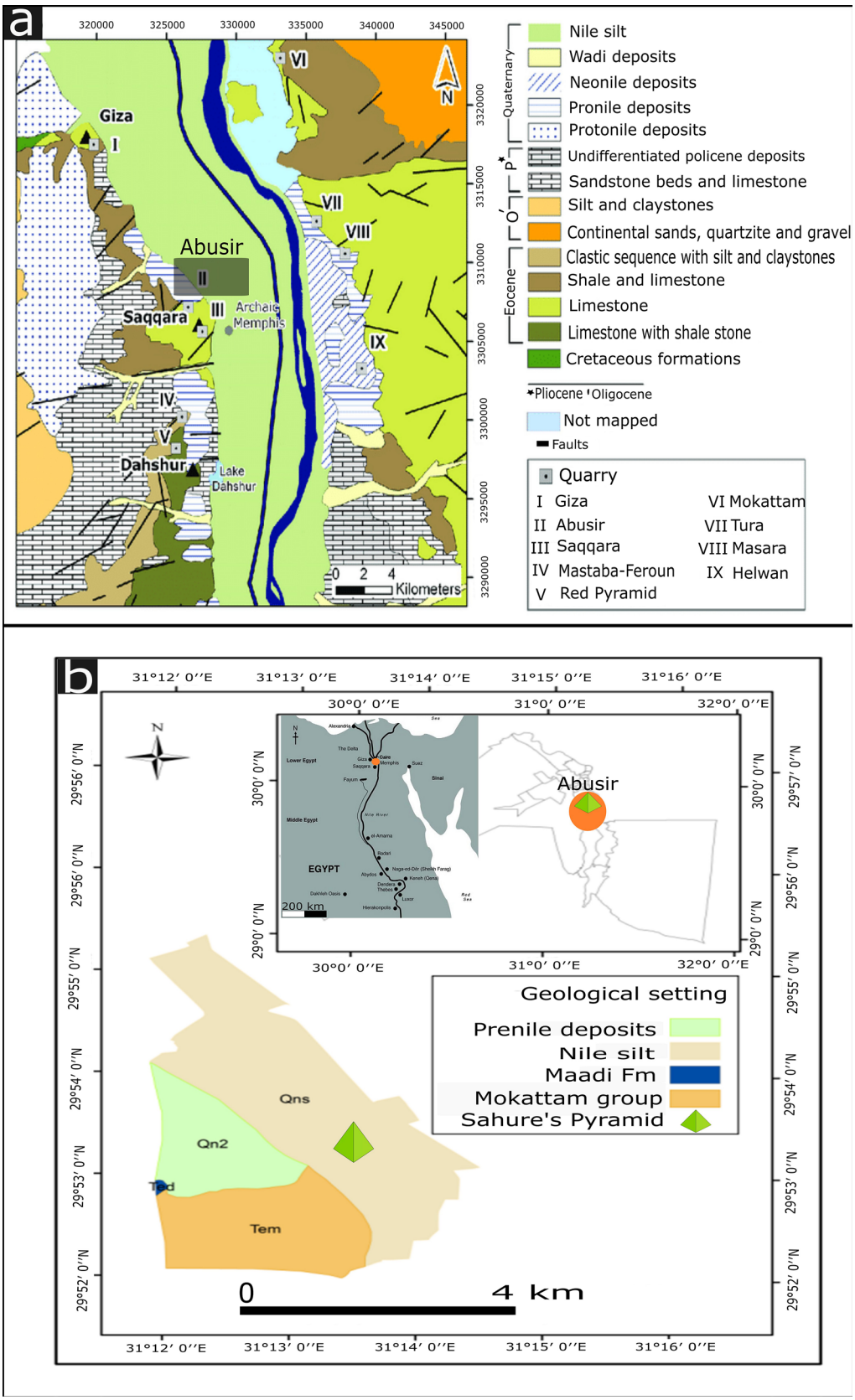

Fig. 3 (See legend on previous page.)

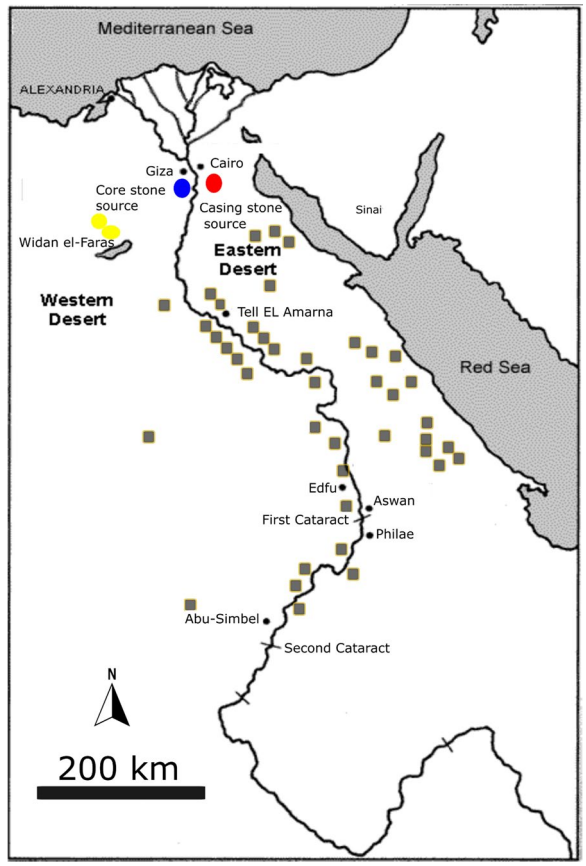

Fig. 4 Map of ancient Egyptian quarries (gray squares). The yellow circle refers to the Widan El-Faras quarry, the red circle refers to the Tura and Massara quarries as the source for casting blocks, and the blue circle is the local quarry of the Abusir site as the source for core blocks

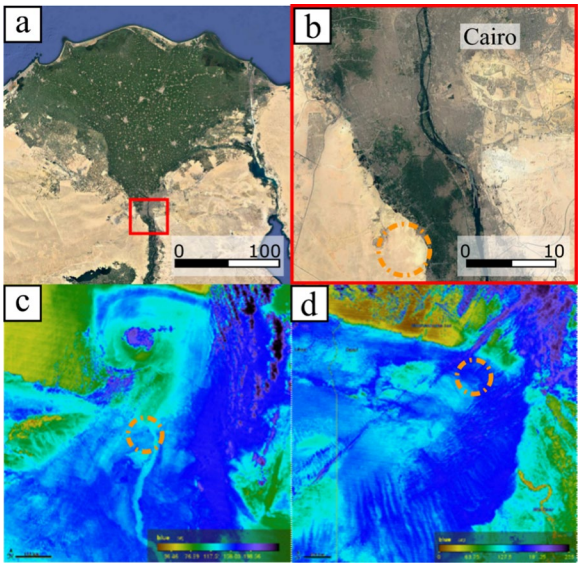

Fig. 5 **a** General map of Egypt, where the red square marks the Abusir zone, referring to the Abusir archaeological site in an orange circle (**b**). **c** The treated satellite image on the NASA Terra satellite (May 2010) explains the dust and sandstorms over Egypt spirally in blue, which extends strongly from the red sea and Nile River to the Mediterranean Sea. The amount of sand and dust thickly exists and results in the total hiding of the land surface below (edited after https://earthobservatory.nasa.gov/images). **d** The treated satellite image from the NASA Terra satellite (April 2012) explains the dust and sandstorms in blue, which extends strongly from north-northeast to south-southwest. The amount of sand and dust is high, resulting in the total hiding of the land surface below (edited after https://earthobservatory.nasa.gov/images)

affect them differently and accelerate the rate of construction material decay.

Geodynamic factors

Egypt was exposed to many historical earthquakes that were recorded and reported from 2200 BCE to 1899 AD. Most of the earthquake epicenters were located in Cairo, and the damage from earthquakes affected Cairo, the Nile Delta, and the Nile valley. For example, in 520 AD, a large one happened, and many cities and villages were swallowed up [58] (Table 1). In 1992, Memphis pyramids were affected by the Dahshour earthquake with an estimated magnitude of 5.3 and depth of 30 km. Thus, geotechnical problems were observed, such as soil settlement and the settlement estimated in some villages at 1.75 km. Accordingly, the most common damage patterns for the buildings were the complete collapse, separations of the buildings, and diagonal cracks [59–61]. Other important examples of earthquake damage can be found in the northern pyramid of Snefru, where structural damage appeared, such as longitudinal structural cracks in the internal chamber [25]. In addition, both the Dahshour and Aqaba earthquakes caused partial collapse of the Step pyramid [22]. Finally, earthquakes also affected the Abusir archaeological site and its pyramids because it is very near the Dahshour site. Accordingly, limestone enclosure walls of the shaft tomb of Udjahorresnet at Abusir were damaged and crumbled [62]. In addition, Sahure's pyramid was damaged, and many features of structural damage that resulted from the earthquakes were monitored.

Materials and methods

Materials

Some fragments of limestone (casing stone) and sandy limestone (core stone) (Fig. 6b) were collected for analysis from the original quarries (Fig. 6a, red circle) to use in the analysis and identification of physical properties. Highly weathered fallen parts were collected for

analysis and examination purposes (Fig. 6a, blue circle). In this sense, samples taken from the quarry are referred to in the text as "unweathered", while those taken from the fallen blocks of the pyramid are called "weathered". Finally, a fragment of mortar was taken from highly weathered fallen parts for its analysis and investigation (Fig. 6c).

Methods

Visual and morphological description

Visual examination was carried out to collect information about the construction materials to identify the specific problems of the different construction materials of the pyramid. Additionally, the morphological examination was performed by using a digital microscope (USB digital microscope with stand), magnification between 20 and 400×, and equipped with a digital camera 1.3 Mpx. In addition, some in situ visits and field work were made to record all problems of the pyramid, structural deficiencies, documentation, and geoenvironmental analysis.

Mineralogical characterization

A polarized light microscope (PLM) was carried out in the central lab of the Egyptian General Authority of Mineral Resources as a mineralogical and petrological analysis for stone samples. It has been used to identify the minerals and to specify the alteration processes of these minerals because of the geo-environmental effects on the building materials of the pyramid. X-ray diffraction (XRD) was utilized to identify the mineralogical content of the core stone, unweathered and weathered casing stone, and basaltic mortar. For that, a few grams of the samples were ground in an agate mortar, and the powders were analyzed using an PW-1480 X-beam diffractometer with the following conditions: CuK_{α} radiation, goniometer speed $2\theta = 1$ degree/min at a steady voltage 40 kV and 30 mA.

On the other hand, the clay fraction was carried out throughout the separation process for clay minerals from core stone. Accordingly, a few grams of core stone powder were prepared and admixed in a solution with 1000 ml of distilled water and 100 ml of acetic acid, followed by stirring the mixture for 20 min every day until no reaction was observed. The clay fraction was collected on three glass slides for analysis. The first slide was considered an oriented untreated aggregate, the second slide was treated using dimethyl sulfoxide, and the third slide was thermally treated at 550 °C for 2 h.

Chemical characterization was carried out by means of X-ray fluorescence (XRF) in the Central Laboratory of Egyptian General Authority of Mineral Resources as an elemental analysis for the stone samples to identify the major and minor elements. Elemental analysis was carried out using an X-ray fluorescence spectrometer on pressed powder pellets to determine the bulk chemistry.

Physical properties

To determine the petrophysical properties, such as specific gravity, apparent density, water absorption, moisture content, and porosity, nine cubic samples were prepared from local sandy limestone at the Abusir archaeological site at 5 × 5 × 5 cm. The samples were weighed naturally after drying at 105 °C, and then the samples were saturated in water to determine the natural weight, dried weight, and saturated weight.

Petrophysical testing was measured and calculated according to IS: 2386 (Part III) [63] and ASTM C97 [64]. The moisture content (MC) of the stone was expressed as a percentage by subtracting the dried weight of the stone from the natural weight and then dividing them by the dried weight according to the formula $MC = (weight_{wet} - weight_{dry})/weight_{dry}*100$ Weight [65]. In addition, water absorption (WA) is expressed as the percent weight change due to absorbed water and calculated according to the formula $WA = (M_{wet} - M_{dry})/M_{dry} \times 100\%$. Moreover, the density (D) of the stone indicates the unit weight of the stone and is calculated by dividing the mass up the total volume of the stone according to the formula $D = m/v$ [66]. Furthermore, unit weight (UW) was calculated by the gravitational force on a mass and is represented by the formula $UW = m*g$, where weight can be $g*mm/s^2$. In addition, Specific Gravity (SG) is the ratio of the density of the stone to the density of water, and the specific gravity of natural stones ranges from 2 to 3 and is expressed as $SG = \rho_{substance}/\rho_{H2O}$. Finally, the porosity (Po) is a measure of void spaces inside stones and was measured according to the formula $Po = V_{V/}V_T$ [67].

Results

In situ investigation

Field observations were carried out to evaluate the current state of preservation, photographing, and recording for all deterioration patterns due to the effect of both

Table 1 Examples of historical earthquakes with their approximate latitudes and intensities

Date	Lat. E	Intensity (MMI)
2200 BC	30.75 (Tell Basta)	VII (destructive)
39 AD	30.20 (Northern Egypt)	VI (very strong)
520 AD	31.00 (Northern Egypt)	VII (destructive)
885 AD	30.10 (Northern Egypt)	VII (destructive)
1847 AD	29.50 (Northern Egypt)	VIII (Very destructive)

Edited after Ref. [58]

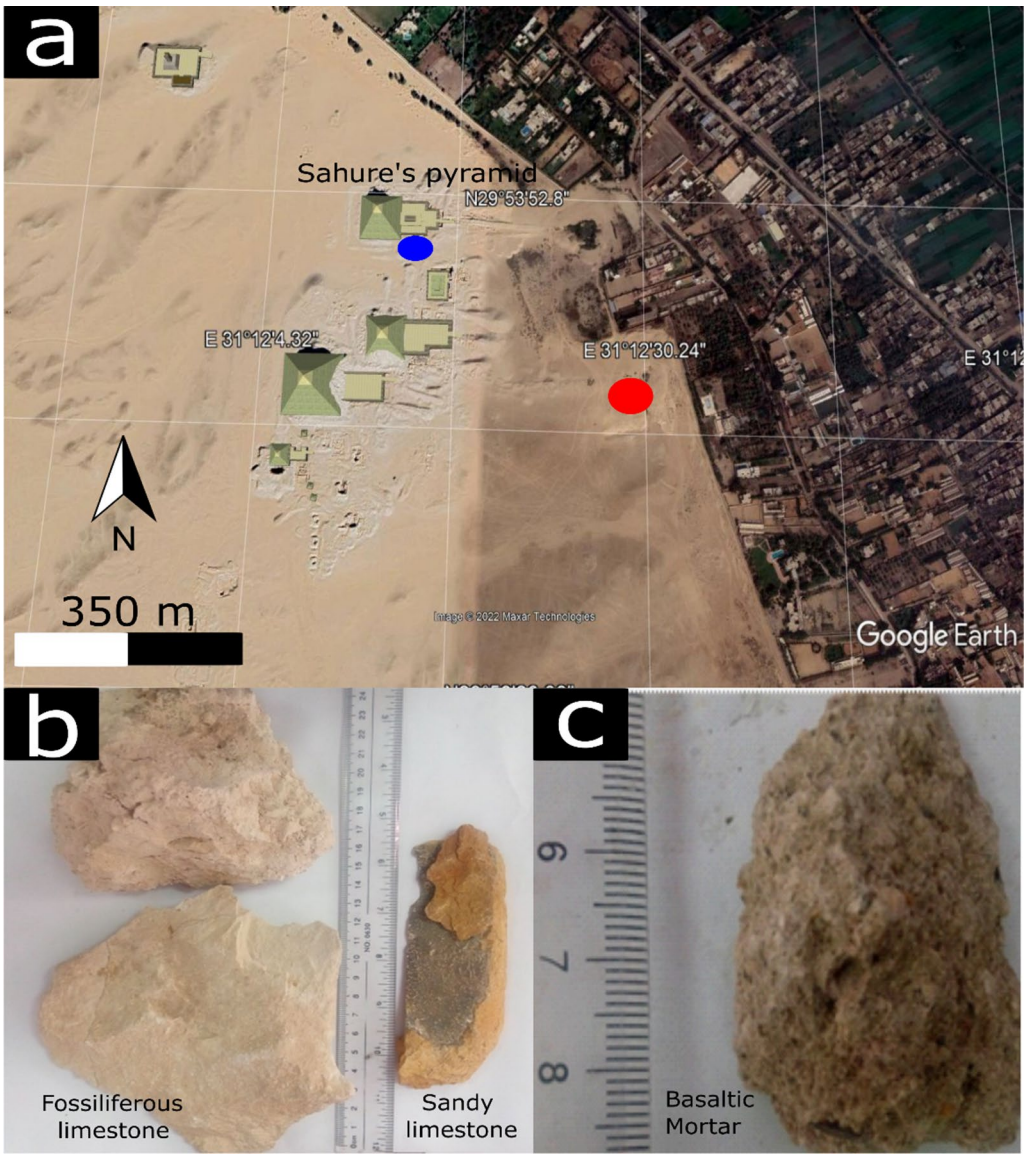

Fig. 6 **a** Image from Google Earth map showing the representative sampling areas for the construction material of the pyramid near Abusir village. The red circle refers to the local quarry from which the core blocks of the pyramid were extracted, and in the blue circle, the place where some fragments were collected from fallen and highly weathered fragments/samples. These fragments represent the fossiliferous limestone as casing stone and sandy limestone as core building material (**b**) and the mortar fragment (**c**)

geoenvironmental and internal (stone properties) deterioration factors. Remarkable structural deformations and damage have been observed, and they were recorded, such as total separation and collapse of casing stones, wall crumbling, and structural damage. The damage has occurred because of the accumulative effects of historical and recent earthquakes with wind stresses (Fig. 7a and b). Visually, the main forms of decay are exfoliation, delamination, scaling, powdering and alveolarization due to wind, wet-dry cycling, rain, and pollution conditions (Fig. 7c, d, e, and f, respectively). Moreover, the degradation form of detachment/layering on construction materials is due to daily exposure to thermal and cooling cycling, which causes the expansion or contraction/shrinkage of minerals of the stone and finally leads to laminations and layering patterns [68].

Macro and microscopic description

A digital microscope was used for the morphological description of the core and casing building stones, as well

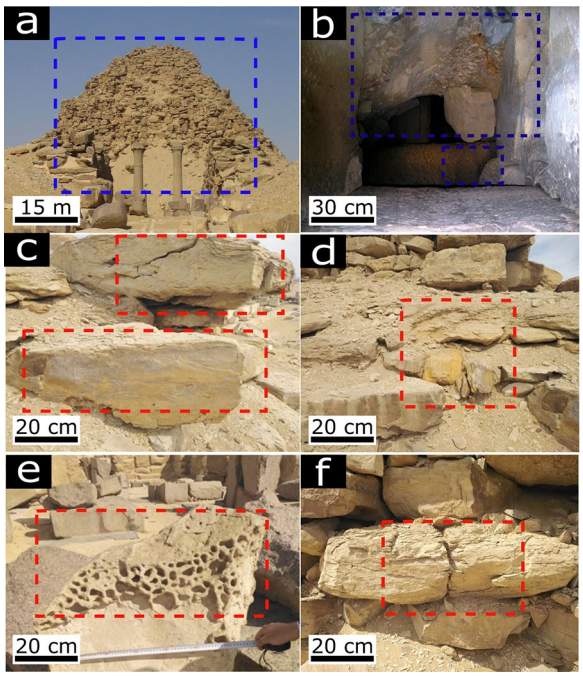

Fig. 7 Features of damage and degradation of Sahure's pyramid building materials. **a** Collapsed blocks from core and casing stones due to earthquakes and environmental impacts (blue rectangle). **b** Structural cracks and crumbling of stone blocks due to earthquakes (blue rectangle). **c** Exfoliation and detachments of the stone blocks (red rectangle). **d** Scaling, powdering, and differential weathering of sandy limestone blocks (red rectangle). **e** Alveolar weathering. **f** Weakening and splitting of stone blocks

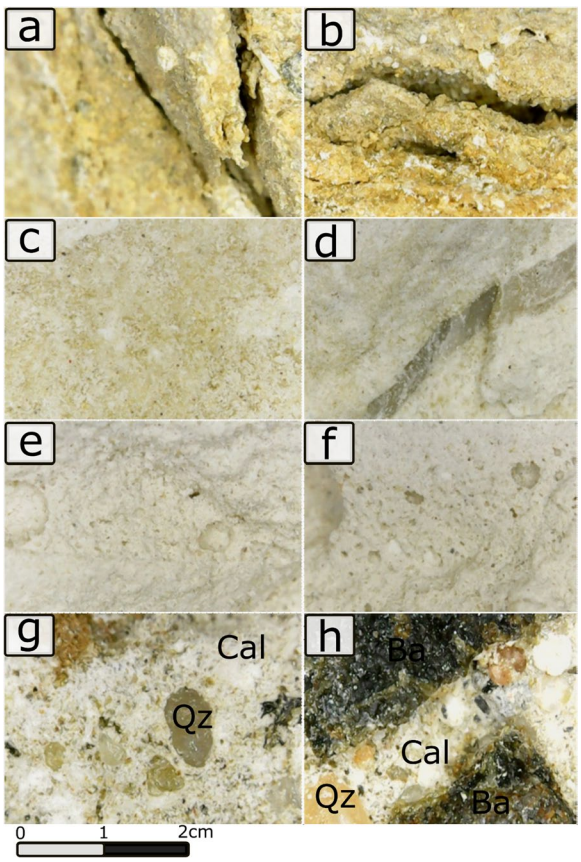

Fig. 8 Microphotographs under the digital microscope for the construction materials of Sahure's pyramid. **a** and **b** Core stone, grains of quartz admixed with calcite, fractures, laminations, and microcracks are detected. **c** and **d** Unweathered casing limestone is a very white stone, microveinlets filled with calcite and quartz are observed, and comb texture is observed in some microveinlets. **e** and **f** Weathered casing limestone of the pyramid with clear irregular pore spaces present in the carbonate matrix of the stone and comb texture is observed. **g** and **h** Sample of mortar with a significant amount of microfossils and fossil fragments are observed in the carbonate samples and in the groundmass, and several irregular interparticle pores are detected in the mortar. Legend: Cal (calcite), Qz (quartz), and Ba (basalt rock fragments)

as the mortar, to study their morphological and textural features, as well as to identify and reveal the deterioration sources and patterns.

The core stone (sandy limestone, Fig. 8a and b) texture of the pyramids is very fine to fine-grained. The stone is laminated due to relative variation in mineral composition and grain sizes and orientations, which reflects the differential behavior towards the geoenvironmental impacts, and this is considered one of the intrinsic problems of the stone body. Some irregular pore spaces and microcracks were detected with a considerable amount of sand grains inside the fractures. Black crusts were observed on the surfaces of stone, and some salts (possibly gypsum) partially fill the pores of the stones as well as cover some areas on the surfaces.

The unweathered casing stone (fossiliferous limestone) of the pyramid is a very white stone (Fig. 8c), with microveinlets filled by calcite and quartz, and comb texture is observed in some of the microveinlets (Fig. 8d). On the other hand, the surface of the weathered casing limestone presented a honeycomb texture due to the dissolution of the carbonate matrix and the production of pores over the surface (Fig. 8e and f).

The mortar sample was examined and showed a fine- to coarse-grained texture, composed of numerous mineral grains, mainly quartz, and rock fragments spread in a very fine-grained matrix (Fig. 8g). Regarding the rock fragments used as sand (grains), apart from quartz and some limestone fragments, others were observed with a very dark color, black to greenish. This color and the crystalline appearance suggest that these fragments may be basaltic rocks (Fig. 8h). Finally, significant irregular interparticle pores were detected in the sample.

Under the polarizing microscope, the core stone (Fig. 9a) is very fine- to fine-grained, essentially

composed of calcite and, as secondary mineralogy, dolomite, clay minerals, and quartz, associated with iron oxides, opaque minerals, and rare amounts of feldspar, glauconite and phosphatic minerals. Carbonates occur as very fine-grained, anhedral to subhedral crystals that represent the matrix of the stone. Clay minerals occur as very fine-grained anhedral aggregates admixed with carbonates. Quartz is present as very fine-to-fine grain crystals scattered in the matrix, and the average grain size of fine quartz is 3 mm**.** Iron oxides are present in minor amounts and related to the clay minerals, as well as disseminated in the stone to be responsible for the reddish or/and yellowish colors. A significant number of microfossils and fossil fragments are observed, and some microfossils are filled with secondary calcite and quartz. Some irregular pores and fractures are detected in the sample, and microveinlets are filled by secondary calcite, quartz, and iron oxides cut across the sample. Dolomite may be present as mineral alternation after calcite (dolomitization process).

For the casing stone, unweathered and weathered samples have been observed. In the first case, the unweathered sample (Fig. 9b) is mainly composed of micritic minerals as the essential component associated with minor amounts of dolomite, rare iron oxides, quartz, phosphate minerals, and opaque minerals. Iron oxides are observed as staining over some parts of the sample due to their dissemination, especially in the presence of humidity or water source, which causes discolouration and disintegration of the stone. Quartz is detected as very fine-grained crystals scattered in the matrix. Phosphate occurs as very fine bone fragments scattered in the stone. Some pores with irregular shapes and various sizes are observed scattered in the rock. Microveinlets are filled with calcite, and quartz is observed cutting through the sample. On the other hand, the weathered sample (Fig. 9c) is composed mainly of micrite and dolomite as the essential components associated with quartz and rare amounts of feldspars, gypsum, opaque minerals, iron oxides, and clay minerals. Quartz occurs as very fine- to fine-grained, anhedral grains scattered in the matrix. Significant amounts of microfossils of different sizes and shapes are scattered in the matrix of the sample, where some of them are filled by secondary sparite. Some parts of the stone are stained by traces of iron oxides. Secondary quartz replaces calcite both in the matrix and in some microfossils. Secondary gypsum replaces calcite and partially fills cavities and pore spaces.

Finally, the mortar is mainly composed of aggregate particles by rock fragments, quartz, and feldspar associated with minor amounts of iron oxides, opaque minerals, and clay minerals cemented by calcite. The matrix appears admixed with gypsum. The observed stone fragments are of sedimentary (limestone, gypsum, or feldspathic graywacke) and igneous (porphyritic basalt and rhyolite) origin. Rock fragments are coarse- to medium-grained and have rounded to subangular shapes. Limestone fragments are the most abundant constituent. They comprise very fine- to fine-grained, subhedral to anhedral-interlocked calcite crystals. Most of the limestone fragments are microfossils of different sizes and shapes (Fig. 9d). Some of the limestone fragments are cut by fine microveinlets filled by secondary calcite. Gypsum rock fragments are composed of a network of very fine-grained irregular gypsum crystals, and the identification of this texture is characteristic of secondary gypsum after anhydrite, which is created where the precursor of anhydrite rehydrated to gypsum [69] (Fig. 9e). Some gypsum fragments are dissolved, leaving relics on the inner border of the secondary pores. Porphyritic basalt fragments in the archaeological sample are generally composed of very fine- to fine-grained plagioclase (anorthite) associated with olivine and/or pyroxene. Plagioclase in these fragments is slightly altered to sericite, while olivine is high to completely altered to iddingsite, which is partially altered to limonite as well. Pyroxene is slightly altered to chlorite and iron oxides (Fig. 9f). Mafic minerals (pyroxene and altered olivine) present as very fine- to fine-grained crystals that are observed in the matrix that reflect strong alterations of the rock fragments and the whole sample. Feldspathic greywacke fragments comprise very fine-to-fine grains of poorly sorted quartz (sand grains) associated with major feldspars and rare mica embedded in a very fine matrix of clay minerals and iron oxides. Ironstone fragments are composed of very fine- to fine-grained quartz and minor calcite embedded in the cement of iron oxides and opaque minerals. Ironstone fragments are generally porous. Rhyolite fragments are the least abundant and are composed of very fine- to fine-grained quartz and potash feldspars (mainly microcline). K-feldspars are slightly altered to clay minerals. Free quartz grains occur as very fine to fine-grained grains with rounded to subangular outlines, and some grains are polycrystalline. Feldspar (anorthite) occurs as fine-grained euhedral to subhedral crystals scattered in the matrix of the sample (Fig. 9f). Calcite occurs as very fine-grained (micrite) aggregates that represent the majority of the matrix of the rock. Iron oxides and opaque minerals occur as very fine- to medium-grained scattered minerals in the sample. Gypsum occurs as very fine-grained, fibrous aggregates to needle-like crystals scattered in the matrix of the sample. Clay minerals occur as very fine-grained admixed with all the matrix components. Some irregular pores and fine fractures are detected in the sample (Fig. 9f).

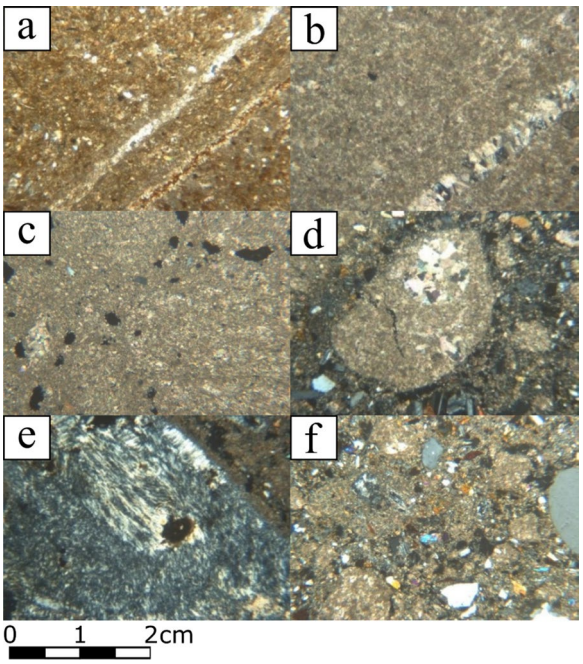

Fig. 9 **a** Thin section for the core stone investigated under the polarizing microscope. The sample shows the pore spaces, channels (microcracks), and dolomite presented as alteration minerals after calcite (dolomitization process). **b** The casing stone under a polarizing microscope. The stone is cut by microveinlets filled with secondary calcite and traces of quartz. Quartz presents as a secondary replacement mineral over carbonates, especially microfossils. **c** The decayed casing stone under a polarizing microscope. Secondary quartz replaces calcite both in the matrix and in some microfossils. Secondary gypsum replaces calcite and partially fills cavities and pore spaces. **d** Observed stone fragments are of sedimentary (fossiliferous limestone, gypsum (chemical alteration byproduct), feldspathic graywacke, and ironstone) and igneous (porphyritic basalt and rhyolite) origin **e** in basaltic mortar. Gypsum rock fragments are composed of a network of very fine-grained irregular gypsum crystals, and this texture is characteristic of secondary gypsum after anhydrite. **f** Some grains of quartz are polycrystalline, feldspar (anorthite) occurs as fine-grained euhedral to subhedral crystals scattered in the matrix, calcite occurs as very fine-grained (micrite), iron oxides and opaque minerals occur as very fine to medium-grained, gypsum occurs as fibrous aggregates to needle-like crystals, and some irregular pore spaces and fine channels are detected

Mineralogical and chemical studies

The mineralogical results of the pyramid construction materials using XRD showed that the core stone sample is composed of calcite (79%), quartz (3%), and dolomite (18%) (Fig. 10, CS) (Table 2, CS). In addition, swellable clay minerals have been detected in the core stone after carrying out the separation process of clay minerals from the core stone powder of the pyramid. We observed that the main peak (with a spacing ≈ 13 Å) moved towards greater spacing when dimethylsulfoxide (≈ 18.6 Å) was applied. In addition, heat treatment was applied and caused the collapse of the structures of these swelling clays, where their spacing decreased to ≈ 9 Å (Fig. 11). Moreover, the unweathered casing stone is composed of calcite (93%) and dolomite (7%) (Fig. 10, UWsC) (Table 2, UWsC), while the weathered casing stone is composed of calcite (80%), dolomite (3%) and quartz (15%) (Fig. 10, WsC) (Table 2, WsC). Finally, the mortar is composed of calcite (40%), gypsum (30%), quartz (10%), and anorthite (20%) (Fig. 10, BM) (Table 2, BM).

Furthermore, all samples were analyzed elementally using X-ray fluorescence, and the identified elements were Ca, Fe, Si, Mg, Al, Na, K, Cl, and Ti (Table 3). The percentage of each element is clearly related to the mineralogy identified by XRD, observing that Ca has similar values. On the other hand, Si and Mg quantities vary more significantly, which is related to the quantities of quartz and dolomite in these rocks. In CS, there is also a contribution of elements related to silicates, such as Al. Likewise, the amount of Fe detected would be linked to the natural variability that these samples present with respect to the Fe oxides described previously. Last, the mortar sample is very different from the rocks. It has much less Ca, but instead the values of Si, Al, Mg, Fe, and K due to the presence of basaltic and rhyolitic rock fragments. Additionally, elements such as P, Cl, and S are present in greater quantities than in rocks, where the presence of P and Cl could be due to the presence of secondary salts and S could be due to the addition of gypsum to the mortar with lime.

Physical properties

Physical properties were measured for the core stone to identify the moisture content (MC), water absorption (WA), density (D), unit weight (UW), specific gravity (SG), and open porosity (Po). To evaluate the durability problems and the geoenvironmental effects on probable changes in stone physical properties.

The results of the physical properties are summarized in Table 4, where the moisture content ranges from 26 to 31.6%, the water absorption ranges from 29.2 to 31.9%, the density is 2.7 g/cm^3, the unit weight is 27 g.mm.s^2, the specific gravity is 2.7 g/cm^3 and the open porosity ranges from 0.7 to 1.6%.

Discussion

The main purpose of this research is to study the effects of geoenvironmental impacts on the sustainability and durability of Sahure's pyramid, as well as to study the interaction process between both intrinsic properties/

defects of the construction materials and surrounding geoenvironmental conditions. Additionally, this research presents a new finding of the oldest trial in the world for mortar/concrete manufacturing, and it is called basaltic mortar/concrete, which is used as joint mortar in pyramid building.

The natural heterogeneity of the sandy limestone that is used in the core construction of the pyramid back to its mineralogical content, such as iron oxides, reflected the reddish or/and yellowish color of the stone and played a role in the accelerating rate of stone decay against environmental conditions. Aggregates of sands admixed with carbonates and clay minerals existed in minor amounts and disseminated in the stone. Additionally, the core building materials have their own internal defects that lead to the weakness of their durability and resiliency towards aggressive and cyclic environmental and weathering impacts, which could be due to thermal stresses, wind, and rain. Petrographical and analytical results showed that the core stone is composed of calcite, dolomite, gypsum, clay minerals, and quartz, associated with minor amounts of iron oxides and opaque minerals and rare amounts of feldspar, glauconite, and phosphate minerals. Among all the mineralogy, the presence and content of phyllosilicates, glauconite, and especially swellable clays suppose a serious risk to the integrity of this natural stone. According to Mahrous [71], both phyllosilicates (smectite and glauconite) are present in the limestone from different quarries in Egypt, and their proportions vary according to the quarry, such as Helwan (1.10%), Qena (0.78%), Minia (0.61%), Assiut (0.60%), Aswan (0.20%), Sinai (0.13%), Sohag (0.55%) and Suez (0.43%). Smectite was detected after the separation process of clay minerals from the core stone powder, and it commonly

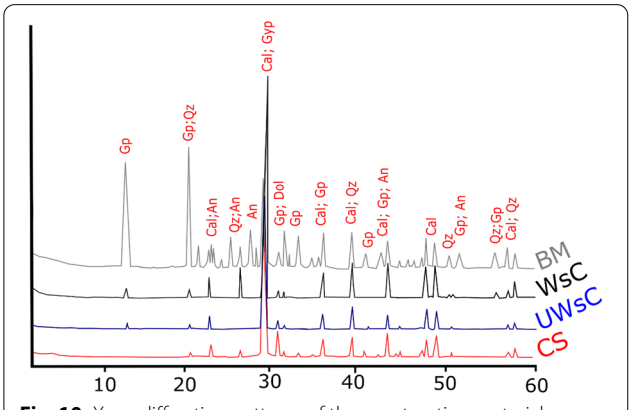

Fig. 10 X-ray diffraction patterns of the construction materials of Sahure's pyramid. Legend: CS, core stone; UWsC, unweathered casing stone; WcS, weathered casing stone; BM, basaltic mortar; Gyp, gypsum; Qz, quartz; Cal, calcite; An, anorthite; Dol, dolomite (according to Ref. [70])

Table 2 XRD results of the core, casing, and basaltic mortar/concrete of the pyramid

	Cal	Dol	Qz	Gyp	An
CS	79	18	3	–	–
UWsC	93	7	–	–	–
WsC	80	3	15	2	–
BM	40	–	10	30	20

CS core stone, *UWsC* unweathered casing stone, *WcS* weathered casing stone, *BM* basaltic mortar, *"-"* a mineral phase not registered, *Cal* calcite, *Dol* dolomit,; *Qz* quartz, *Gyp* gypsum

An anorthite (according to Ref. [70])

exists in sandstones and is characterized by specific physicochemical properties, such as a highly active surface with high cation exchange properties due to its structure, chemical composition, and small crystal sizes [72–74]. Consequently, smectite has a large affinity for absorbing water from the surrounding environment, especially montmorillonite, which causes severe decay for the pyramid building material due to its shrinkage and swelling characteristics [75]. In this sense, Tiennot et al. [76] studied and confirmed the influence of smectite and glauconite on stone monuments and found that low moisture content has a high impact on swelling action to smectite and glauconite, and they assured that under normal environmental conditions, those clay minerals could cause clear weakness planes in the stones. Accordingly, the core stone of the pyramid with its content of swellable clays showed its weakness against changeable environmental conditions, especially in the fluctuation between temperature and humidity conditions. In addition to the heavy rains and wind loads that led to detachments, layering, and delamination, partial and total structural collapse occurred with dynamic actions. These previous deterioration patterns are considered the main decay patterns in the building materials of the pyramid (see Fig. 7). Furthermore, iron oxides were detected as minor impurities in the chemical composition of the core stone, and in correlation with previous studies, clay minerals rich in iron oxides existed in the composition of the samples of limestone from Al-Zahir Baybars Mosque in Old Cairo. In fact, they were the reason for the reddish color of the stones, and iron oxides dissolved in the water source of sewage caused many patterns of decay, such as powdering and disintegration of stone blocks [77]. Accordingly, the color of the core stone is strongly reddish, and because of the dissolution process, the stones are full of pores, microcracks, and laminations.

Moreover, in Giza, many pollutants are observed with increasing rates from September to November, such as carbon monoxide, nitrogen oxides, ozone, and sulfur

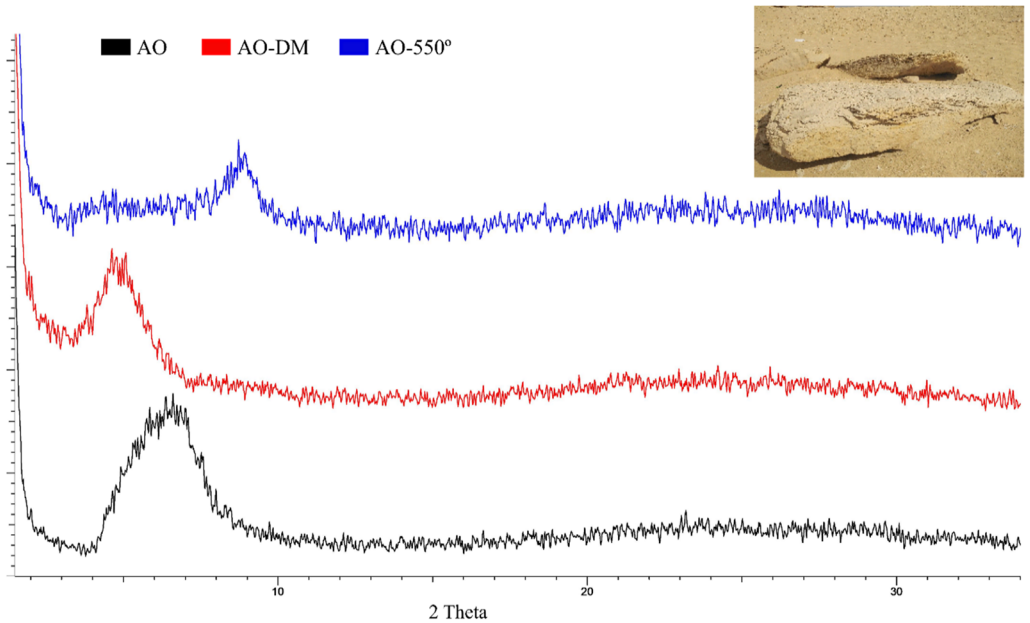

Fig. 11 X-ray diffraction patterns of the clay fraction from the core stone sample, where the main peak observed corresponds to swellable clays. The AO sample (black line) corresponds to oriented aggregates without treatment, AO-DM (red line) after treatment with dimethyl sulfoxide, and finally, AO-550° (blue line) treated thermally at 550 °C

Table 3 Chemical composition of the core stone, unweathered and weathered casing stones, and basaltic mortar from Sahure's pyramid

	CaO	SiO_2	TiO_2	Al_2O_3	Fe_2O_3	MnO	MgO	Na_2O	K_2O	P_2O_5	Cl	SO_3	LOI
CS	47.90	4.80	0.10	0.40	5.10	0.09	2.40	0.09	0.06	0.02	0.23	0.69	37.90
WCS	53.22	1.90	0.10	0.11	0.50	0.03	1.18	0.07	0.06	0.08	0.18	0.66	41.80
UWCS	52.74	3.54	0.12	0.18	0.52	0.01	1.10	0.04	0.01	0.01	0.19	0.69	40.50
BM	31.19	18.80	0.80	3.79	7.93	0.10	0.97	0.12	0.90	0.14	0.40	16.9	17.50

Major and minor elements are expressed in wt. %

CS core stone, *WCS* weathered casing stone, *UWCS* unweathered casing stone, *BM* basaltic mortar

dioxide [55]. Accordingly, gypsum byproducts appear in core stone with 2% because of the reaction of calcium carbonate with sulfuric acid as an environmental pollutant [78]. In the same context, gypsum salt is formed inside the porous building materials due to the accumulative reaction between sulfuric acid and calcium carbonate that leads to irreversible damage to the stones, and the internal fabric of the stone is replaced with gypsum [79, 80]. In addition, the presence of dolomite might have occurred because of the dolomitization process originally, where the limestone was altered into dolomite when the stone was in contact with water rich in magnesium, and this transformation was accompanied by an increase in porosity [81].

Since the two components of calcite and quartz have existed, it is expected that the differential thermal expansion rates will be different, which could cause many internal stresses leading to microcracks, fissures, and disintegration for the stones. In particular, the thermal coefficient volumetric expansion of quartz is 0.36 between 20 and 100 °C; calcite shows anisotropic thermal strain behavior due to its positive and negative linear thermal expansion coefficients. These different coefficients generate high tensile stresses along crystal boundaries, significantly impacting the disintegration of stones in the high frequency of fluctuations of the temperature daily and monthly. Similar to calcite, dolomite is present in the core stone, and they have different thermal expansion coefficients [82, 83]. Accordingly, many deterioration patterns, such as layering and cracking, could be noticed because of the various thermal expansion coefficients of different minerals in the core building materials.

On the other hand, ancient Egyptians utilized limestone from ancient quarries (Tura and Massra quarries)

Table 4 Results of the petrophysical properties for the core stone (sandy limestone) of the pyramid

Sample No.	1	2	3	4	5	6	7	8	9
L	5.0	5.0	4.7	5.0	4.9	4.7	5.0	5.0	5.0
W	5.0	4.8	5.0	5.0	5.0	5.0	5.0	4.8	5.0
H	4.8	5.0	4.7	5.0	5.0	5.0	5.0	5.0	5.0
V	120.0	120.0	110.5	125.0	122.5	117.5	125.0	120.0	125.0
M	324.0	324.0	298.3	337.5	330.8	317.2	337.5	324.0	337.5
NW	291.8	307.3	306.3	319.7	315.2	297.05	300.3	302.2	317.3
DW	292	306	306	318.5	314.3	296	299	301	316
SW	293	307	307.2	319.4	315.2	297	300	303	317.4
MC	26	30.6	30.5	31.9	31.4	29.6	30	30.1	31.6
WA	29.2	30.6	31.6	30.9	31.5	29.6	30	30.2	31.7
D	2.7	2.7	2.6	2.7	2.7	2.6	2.7	2.7	2.7
UW	27	27	26	27	27	26	27	27	27
SG	2.7	2.7	2.6	2.7	2.7	2.6	2.7	2.7	2.7
Po	0.8	0.8	1.0	0.7	0.7	0.8	0.8	1.6	1.1

L length (in cm), *W* width (in cm), *H* height (in cm), *V* volume (in cm^3), *M* mass (in g), *NW* natural weight (in g), *DW* dry weight (in g), *SW* saturated weight (in g), *MC* moisture content (in %), *WA* water absorption (in %), *D* density (g/cm^3), *UW* unit weight ($g.mm.s^2$), *SG* specific gravity (g/cm^3), *Po* open porosity (in %)

that were typically light gray on unweathered surfaces but were also nearly white or pale yellowish to pinkish [84]. Accordingly, the unweathered casing stone of Sahure's pyramid is mainly calcite (93%) with some dolomite that was extracted from the Tura and Massra quarries in Helwan. This casing stone is relatively soft due to its abundance of calcite and relatively porous due to some impurities, such as iron oxides, quartz, a phosphate mineral, and opaque minerals. Limestone owes its own hardness to either more coarsely crystalline calcite or the presence of secondary dolomite as the casing stone of the pyramid [85]. Tura and Massra stones consist mainly of calcite. In addition, they contain fossils (molluscs, and especially echinoids and globigerinid, nummulite foraminifera, *Ostreaelegans*, *Pectens. p*, *Lucina mokattamensis*) plus one or more of the following impurities: dolomite, quartz (as detrital sand silt grains or diagenetic chert nodules); iron oxides (hematite or goethite) and various clay minerals (aluminosilicates). In contrast, the weathered samples of casing stone are composed mainly of calcite and dolomite as the essential components associated with a few amounts of quartz and traces of feldspars, gypsum, biotite, opaque minerals, iron oxides, and clay minerals. Secondary quartz replaces calcite, and some parts of the stone are stained by traces of iron oxides. Additionally, secondary gypsum is also replacing calcite because of a chemical weathering reaction between pollutants and calcium carbonate leading to partial cavities and pore spaces.

For the mortar and after petrographical and analytical studies, the results showed that it is affected by a slight alteration over essential mineral constituents. Some microfossils are filled by secondary calcite, and limestone fragments are occasionally cut by fine microveinlets filled by recrystallized secondary calcite. Gypsum fragments are generally secondary after anhydrite because of acidic rains. In this context, Sievert et al. [86] confirmed the conversion of anhydrite into gypsum during hydration when anhydrite is exposed to a water source and water molecules enter through the cracks of the anhydrite surface. In addition, when there are sufficient Ca^{2+} and SO_4^{2-} ions and water molecules at the surface, nuclei of gypsum are formed. Finally, a large amount of gypsum is formed, and the remaining anhydrite is left behind. Furthermore, some gypsum fragments are dissolved, leaving relics on the inner border of the secondary pores in the mortar. In this sense, gypsum can be soluble and dissolved in the presence of an unsaturated aqueous solution releasing Ca^{2+} and SO_4^{2-} ions due to the chemical characteristics of gypsum [87]. Moreover, sericite was detected as an alteration of plagioclase (in fragments and free crystals), and sericite is a common alteration mineral of orthoclase or plagioclase feldspars in regions that are subject to thermal alteration; this process is called sericitization [88]. However, olivine (in fragments and free crystals) is high to completely decomposed to iddingsite and then partially altered to limonite. In this regard, Smith et al. [89] confirmed that olivine is the most reactive mineral under both thermal and weathering conditions. The formation of the iddingsite by oxidative weathering and olivine begins with a solution of Mg from planar fissures, and the oxidation of Fe within the remaining olivine provides nuclei for the growth of goethite. In addition, pyroxene

(in fragments and free crystals) is slightly altered to chlorite and iron oxides.

From petrophysical measurements for the core stones, the water absorption coefficient ranged from 29.2% to 31.7%, the average density was 2.7 g/cm3, the average specific gravity (GS) was 2.7 (g/cm^3) and the open porosity ranged from 0.8 to 1.1% (Table 4). Water absorption of stones is categorized into low-absorbing stone (1 to 10%), moderate-absorbing stone (10 to 50%), and high-absorbing stone (50 to 100%) [90]. According to the physical properties, core stones of the pyramid are categorized as moderately absorbed stones [90]. Water absorption is considered the most important physical property that has relationships with density and porosity due to the reaction of water with the internal composition of stones leaving pores and spaces because of the alterations and dissolution processes. Finally, when the degree of water saturation and absorption increase, the durability of stones decreases [90, 91].

Furthermore, and according to the recordings of historical seismological data, shear forces due to previous earthquakes have affected the pyramid structure. The most important factor that effectively caused major deterioration and structural problems of the Red pyramid near the Abusir archaeological site was the impact of the accumulative earthquakes [25]. Specifically, in 1992, an earthquake occurred at Dahshur with an estimated local magnitude of 5.3 M on the Richter scale [25]. This earthquake caused notable crumbling, casing and body stone collapsing, and structural cracks in Sahure's pyramid. The previous environmental weathering and bleeding of the construction materials helped the damaging impact of the earthquake on the pyramid.

Finally, this study revealed that the first trial for mortar/concrete manufacturing in the world dates back to 2494 to 2345 BCE. In this sense and according to previous studies, the oldest mortar was made from mud and clay back to the 10th millennia BCE. On the other hand, concrete manufacturing dates back to 1400–1200 BCE in the royal palace of Tiryns (Greece). This concrete was composed of lime and pebbles, and small usages of it have been recorded in some structures in the ancient Nabataea culture as well [92]. The name of our study mortar is called basaltic mortar/concrete, and the main precursors of this concrete are basalt and limestone fragments with lime and gypsum. The source area of basalt fragments is the Widanel-Faras quarry, which was referred to in part of the ancient Egyptian quarries (Fig. 4, yellow circle). This kind of mortar/concrete gives more attention to the impressive mentality of ancient Egyptians in the technology of building materials for their pyramids.

Preservation proposal for the pyramid

Sahure's pyramid has been affected by many factors of deterioration (physical, mechanical, and chemical). Many fallen stone blocks and loss of cohesion of construction materials are well observed. Therefore, urgent restoration and conservation are needed to safeguard this important pyramid. The preservation plan should include the fine restoration, structural interventions, preventive conservation, and management of the archaeological site of Abusir. For protection, the dust over the whole body of the pyramid is cleaned, salts are removed from the stone surfaces, stone blocks are consolidated, the gaps are filled, and grouting is performed by using improved traditional mortars such as lime mortar. Finally, a replacement for highly weathered blocks with new blocks is highly needed in most of the pyramid parts.

For structural intervention, the authors suggest carrying out geotechnical studies to investigate structural problems and assessment for the soil problems as well using finite element modelling to specify the areas of deficiencies. In this sense, urgent design for steel or wooden supports for the structural stability of inner chambers is recommended to prevent structural collapse.

Last, the site management plan for the Abusir archaeological site should be carried out for sustainability and preventive conservation purposes. Abusir is listed as a world heritage site with all of Memphis, but very few tourists and researchers go there due to the lack of infrastructure, services, and maintenance. After the development plan for the site, it will be strongly a significant and competitive destination for the tourism industry and researchers in Egypt.

Conclusions

Intrinsic problems related to the mineralogical composition of the construction materials of Sahure's pyramid played an important role in the decay and degradation of these building stones. Clay minerals in core stones, such as smectite and glauconite, affected the durability of the stones due to the swelling force of these clay minerals. Moreover, the paper showed that one of the internal defects of the pyramid construction materials is the original pores in the stone resulting from the dolomitization process of calcite. In addition, pores and spaces are present due to weathering agents and environmental interactions with construction materials. Additionally, gypsum salt replaced calcite and partially filled pore spaces inside stones to form crusts over the stone surfaces and weaken the resiliency of the stones. On the other hand, the presence of anhydrite has been detected because of the high thermal impact of the surrounding environment. The secondary phase of gypsum

from anhydrite has been detected due to the chemical decay of construction materials. Moreover, disseminated iron oxides with humidity caused the staining that made the stones visible as reddish or/and yellowish. In addition, the dissemination of the iron oxides caused pores and spaces because of their dispersion in water. Different thermal behaviors of calcite, quartz, and dolomite affected the durability of the stones, causing disintegrations and layering degradation patterns for the building blocks of the pyramid. Meanwhile, the wind and wet-drying cycle's effects caused the honeycomb decay pattern in some blocks. Petrophysically, the stones have been affected by environmental conditions and categorized as moderate water-absorbing, which makes stones so susceptible to future environmental impacts. Dynamically, the research discussed that the environmental impacts and intrinsic problems were not only the factors of decay and damage but also the accumulative effect of historical earthquakes. Dahshour earthquake (1992), which is adjacent to the Abusir archaeological site, and the Aqaba earthquake (1995) both led to a partial collapse and structural damage of the Sahure's pyramid. Additionally, the paper investigated and confirmed that the core stone of the pyramid is from a local quarry and that the casing stones were extracted from the Tura and Massara quarries. Finally, this work revealed a new discovery related to basaltic mortar/concrete that was the first trial of concrete fabrication in the Old Kingdom in Egypt.

Acknowledgements
A. Fahmy acknowledges SCiCYT and UGEA-PHAM at Cadiz University for carrying out the main part of the archaeometrical analysis. E. Molina Piernas acknowledges co-funding from the European Social Fund (D1113102E3) and Junta de Andalucía.

Author contributions
The whole database construction, investigation, and analysis are presented in the manuscript and were carried out by the first author. Other authors reviewed and supervised the paper. All authors read and approved the final manuscript.

Funding
The authors confirm that A. Fahmy is not currently in receipt of any research funding relating to the research presented in this manuscript.

Availability of data and materials
Data sharing is not applicable to this article, as no datasets were generated or analyzed during the current study.

Declarations

Competing interests
The authors declare that they have no competing interests.

Author details
[1]Department of Earth Sciences, Faculty of Sciences, University of Cadiz, Campus Río San Pedro, 11510 Puerto Real, Spain. [2]Conservation Department, Faculty of Archaeology, Cairo University, Giza 12613, Egypt.

Received: 5 January 2022 Accepted: 21 April 2022
Published: 17 May 2022

References

1. Camuffo D, Fernicola V, Bertolin C. Basic Environmental Mechanisms Affecting Cultural Heritage: Understanding deteriorations mechanisms for conservation purposes. 1st ed. Brussels: Nardini editore; 2010. https://www.cost.eu/publication/basic-environmental-mechanisms-affecting-cultural-heritage-understanding-deterioration-mechanisms-for-conservation-purposes/. Accessed 20 Jan 2022.
2. Charola AE, Pühringer J, Steiger M. Gypsum: a review of its role in the deterioration of building materials. Environ Geol. 2007;52(2):207–20. https://doi.org/10.1007/s00254-006-0566-9.
3. Fitzner B, Heinrichs K. Damage diagnosis at stone monuments—weathering forms, damage categories and damage indices. Acta Univ Carol Geol. 2001;45(1):12–3.
4. Grossi CM, Brimblecombe P. Effect of long-term changes in air pollution and climate on the decay and blackening of European stone buildings. Geol Soc Spec Publ. 2007;271(1):117–30. https://doi.org/10.1144/GSL.SP.2007.271.01.13.
5. Figueiredo MO, Silva TP, Veiga JP. Analysis of degradation phenomena in ancient, traditional and improved building materials of historical monuments. Appl Phys A Mater Sci Process. 2008;92(1):151–4. https://doi.org/10.1007/s00339-008-4466-6.
6. Sandrolini F, Franzoni E, Sassoni E, Diotallevi PP. The contribution of urban-scale environmental monitoring to materials diagnostics: a study on the Cathedral of Modena (Italy). J Cult Herit. 2011;12(4):441–50. https://doi.org/10.1016/j.culher.2011.04.005.
7. Khanlari G, Sahamieh RZ, Abdilor Y. The effect of freeze–thaw cycles on physical and mechanical properties of Upper Red formation sandstones, central part of Iran. Arab J Geosci. 2014;8(8):5991–6001. https://doi.org/10.1007/s12517-014-1653-y.
8. Derluyn H, Vontobel P, Mannes D, Derome D, Lehmann E, Carmeliet J. Saline water evaporation and crystallization-induced deformations in building stone: insights from high-resolution neutron radiography. Transp Porous Media. 2018;128(3):895–913. https://doi.org/10.1007/s11242-018-1151-x.
9. Hemeda S. Geotechnical modelling of the climate change impact on world heritage properties in Alexandria, Egypt. Herit Sci. 2021. https://doi.org/10.1186/s40494-021-00547-8.
10. Risdonne V, Hubbard C, Puisto J, Theodorakopoulos C. A multianalytical study of historical coated plaster surfaces: the examination of a nineteenth-century V and A cast of a tombstone. Herit Sci. 2021. https://doi.org/10.1186/s40494-021-00533-0.
11. Villacreses JP, Granados J, Caicedo B, Torres-Rodas P, Yépez F. Seismic and hydromechanical performance of rammed earth walls under changing environmental conditions. Constr Build Mater. 2021;300: 124331. https://doi.org/10.1016/j.conbuildmat.2021.124331.
12. Hatır E, Korkanç M, Schachner A, İnce İ. The deep learning method applied to the detection and mapping of stone deterioration in open-air sanctuaries of the Hittite period in Anatolia. J Cult Herit. 2021;51:37–49. https://doi.org/10.1016/j.culher.2021.07.004.
13. Emery KO. Weathering of the Great Pyramid. J Sediment Res. 1960;30(1):140–3. https://doi.org/10.1306/74D709DE-2B21-11D7-8648000102C1865D.
14. Hanafy Holail M. Diagenesis of the middle Eocene "nummulite bank" of The Giza pyramids plateau, Egypt: petrologic and 18°/16° evidence. Qatar Univ Sci J. 1994;14(I):146–52.
15. Reader CD. A Geomorphological Study of the Giza Necropolis, with implications for the development of the site. Archaeometry. 2001;43(1):149–65. https://doi.org/10.1111/1475-4754.00009.
16. Pyramids Plateau Groundwater Lowering Activity. Environmental Assessment Report, United States Agency for International Development. USAID Egypt, 2010. https://pdf.usaid.gov/pdf_docs/PA00HS7G.pdf. Accessed 25 Feb 2022.
17. Gandah AF. The Conservation Status of the Pyramid of Khufu. Hist Res Lett 2015;26:12–22.

18. Franc Z. Petrographic observations of the building stones of the great pyramid of Giza. J Eng Geol. 2017. https://doi.org/10.17265/2328-2193/2017.04.002.
19. Hemeda S. Geotechnical modelling of the climate change impact on world heritage properties in Alexandria, Egypt. Herit Sci. 2021;9(1):1–32. https://doi.org/10.1186/s40494-021-00547-8.
20. Madkour FS, Khallaf MK. Degradation processes of Egyptian faience tiles in the step pyramid at Saqqara. Proced Soc. 2012;68:63–76. https://doi.org/10.1016/j.sbspro.2012.12.207.
21. Kukela A. Assessment of stone material deterioration of the exposed surfaces of the step pyramid in Saqqara. Earth Sci Eng. 2013;3:238–44.
22. Khalil AE, Abdel Hafiez HE, Girgis M, Taha MA. Earthquake ground motion simulation at Zoser pyramid using the stochastic method: A step toward the preservation of an ancient Egyptian heritage. NRIAG J Astron. 2017;6(1):52–9. https://doi.org/10.1016/j.nrjag.2016.11.003.
23. Rossi C. Aristotle's mirror: combining digital and material culture. ISPRS Int Archs Photogramm Remote Sens Spat Inf Sci. 2019;42(11):1025–9. https://doi.org/10.5194/isprs-Archives-XLII-2-W11-1025-2019.
24. Ahmed G. Using smart technology in conservation of the ancient Egyptian monuments from environmental impacts. Artic J Urban Res. 2021;5(40):78–97. https://doi.org/10.21608/JUR.2021.31603.1003.
25. Hemeda S, Fahmy A, Sonbol A. Geo-environmental and structural problems of the first successful true pyramid, (Snefru Northern Pyramid) in Dahshur, Egypt. Geotech Geol Eng. 2018;37(4):2463–84. https://doi.org/10.1007/s10706-018-00769-x.
26. Hawass Z. The treasures of the pyramids. In: Accomazzo L, Fabianis VM, editors. White Star. S.R.L. Vercelli. 2003. https://gizamedia.rc.fas.harvard.edu/documents/hawass_treasures_282-285.pdf. Accessed 21 Jan 2022.
27. New Discoveries in the Abusir pyramid field. https://egypte.xsbb.nl/viewtopic.php?t=786663. Accessed 21 Jan 2022.
28. Verner M. Abusir. L'annuaire Coll Fr. 2012;1(111):897–900. https://doi.org/10.4000/annuaire-cdf.1799.
29. Bárta M, Coppens F, Krejčí J. Abusir And Saqqara in the year. Proceedings of the conference held in Prague. Czech Institute of Egyptology, Faculty of Arts, Charles University in June 22–26.2015. https://cegu.ff.cuni.cz/wp-content/uploads/sites/50/2022/01/2021_Abusir_Saqara_2020.pdf. Accessed 25 Jan 2022.
30. Abusir VM. The Necropolis of the sons of the sun. 2nd ed. Cairo: AUCPress; 2017.
31. Kawae Y, Yasumuro Y, Kanaya I, Dan H, Chiba F. Abusir 3D survey Univerzita Karlova, Filozofická fakulta. https://core.ac.uk/display/156980921. Accessed 26 Jan 2022.
32. Verner M. the pyramids. Their archaeology and history. 1th ed. London: Grove Atlantic Ltd; 2002. https://www.meretsegerbooks.com/pages/books/M4134/verner-miroslav/the-pyramids-their-archaeology-and-history. Accessed 26 Jan 2022.
33. Verner M. Forgotten pharaohs. Lost pyramids: Abusir.1st ed. Prague: Škodaexport Academy; 1994. https://www.meretsegerbooks.com/pages/books/M1683/verner-miroslav/abusir-forgotten-pharaohs-lost-pyramids. Accessed 26 Jan 2022.
34. Lehner M. The Complete Pyramids: Solving the ancient mysteries. 1th ed. New York: Thames and Hudson; 2008. https://www.pdfdrive.com/the-complete-pyramids-solving-the-ancient-mysteries-d187727359.html. Accessed 26 Jan 2022.
35. Borchardt L. Das Grabdenkmal des Königs Sáḥu-reʿ (Ausgrabungen der Deutschen Orient-Gesellschaft in Abusir 1902–1908). Univ Bibl Leipzig Hinrichs. 1982. https://doi.org/10.11588/diglit.3364.
36. Wilson JA. The pyramids of Egypt. I.E.S Edwards. J Near East Stud. 1948. https://doi.org/10.1086/370872.
37. Rainer S. Die Ägyptischen Pyramiden: vom Ziegelbau zum Weltwunder. 3rd ed. Zabern: Mainz am Rhein; 1997. http://www.gizapyramids.org/pdf_library/stadelmann_pyramiden_80-158.pdf. Accessed 25 Jan 2022.
38. Bárta M. Abusir in the Third Millennium BC. 2015. https://cegu2.ff.cuni.cz/en/research/projects/field-projects/abusir/abusir-in-the-third-millennium-bc/. Accessed 08 Mar 2022.
39. Bebermeier W, Alexanian N, Blaschta D, Ramisch A, Schütt B, Seidlmayer SJ. Analysis of Past and Present Landscapes Surrounding the Necropolis of Dahshur. J Geogr Soc Berlin. 2011;142(3):325–52.
40. Heldal T, Bloxam E, Storemyr P, Kelany A. The Geology and Archaeology of the Ancient Silicified Sandstone Quarries at Gebel Gulab and Gebel Tingar. Marmora an Int J Archaeol Hist Archaeom Marbles Stones. 2005; 1:11–35. https://www.torrossa.com/en/catalog/preview/2242664. Accessed 25 Jan 2022.
41. Harrell JA, Storemyr P. Ancient Egyptian quarries—an illustrated overview. Geol Soc Spec Publ. 2009;12:7–50. https://www.ngu.no/upload/Publikasjoner/Special%20publication/SP12_s7-50.pdf. Accessed 25 Jan 2022.
42. Bloxam E. Quarries and mining (stone). 2010. http://digital2.library.ucla.edu/viewItem.do?ark=21198/zz0026jkd5. Accessed 12 Mar 2022.
43. Laukamp LC. The pyramids of Egypt. Hispanic Baroque Ekphrasis. 2020. https://doi.org/10.2307/j.ctv16km07k.12.
44. Klemm DD. The stones of the pyramids: provenance of the building stones of the Old Kingdom pyramids of Egypt - University of Missouri Libraries. http://link.library.missouri.edu/portal/The-stones-of-the-pyramids--provenance-of-the/2y73ukLuBH4/. Accessed 21 Jan 2022.
45. Jana D. Evidence from detailed petrographic examinations of casing stones from the great pyramid of Khufu, a natural limestone from Tura, and a man-made (Geopolymeric) limestone. International Cement Microscopy Association—29th International Conference on Cement Microscopy. 2007:206–265. https://anarkia333data.center/livre/evidence-detailed-petrographic-examinations-casing-stones-great-pyramid-khufu-natural. Accessed 19 Jan 2022.
46. Harrell JA. Mapping the Tura-Masara Limestone Quarries. Journal of the American research center in Egypt. 2016;52:199–214. https://lockwoodonlinejournals.com/index.php/jarce/article/view/76. Accessed 21 Jan 2022.
47. Bloxam E, Storemyr P. Old Kingdom Basalt Quarrying Activities at Widan El-Faras Northern Faiyum Desert. J Egypt Archaeol. 2002;88(1):23–36. https://doi.org/10.1177/030751330208800103.
48. World Bank Group. Climate Risk Profile: Egypt. 1818 H Street NW, Washington, DC 20433, 2020. https://climateknowledgeportal.worldbank.org/sites/default/files/2021-01/15723WB_Egypt%20Country%20Profile-WEB.pdf. Accessed 21 Jan 2022.
49. Egyptian Environmental Affairs Agency. Egypt Third National Communication under the United Nations Framework Convention on Climate Change. 2016. https://unfccc.int/sites/default/files/resource/TNC%20report.pdf. Accessed 25 Jan 2022.
50. Masria A. Climate change at Egypt. SciFed Global Warm. 2017. https://doi.org/10.23959/sfjgw-1000009.
51. Ito WH, Scussiato T, Vagnon F, Ferrero AM, Migliazza MR, Ramis J, et al. On the thermal stresses due to weathering in natural stones. Appl Sci. 2021;11(3):1188. https://doi.org/10.3390/app11031188.
52. Abdel-Shafy HI, El-Saharty AA, Regelsber M, Platzer C. Rainwater in Egypt: quantity, distribution and harvesting. Mediterr Mar Sci. 2010;11(2):245. https://doi.org/10.12681/mms.75.
53. Climate change Profile in Egypt. 2019. https://www.government.nl/documents/publications/2019/02/05/climate-change-profiles. Accessed 11 Mar 2022.
54. Charola AE. Stone deterioration characterization for its conservation. Geonomos. 2017;24(2):16–20. https://doi.org/10.18285/geonomos.v24i2.836.
55. Aboel Fetouh Y, El Askary H, El Raey M, Allali M, Sprigg WA, Kafatos M. Annual patterns of atmospheric pollutions and episodes over Cairo Egypt. Adv Meteorol. 2013. https://doi.org/10.1155/2013/984853.
56. Graue B. Stone deterioration and replacement of natural building stones at the Cologne cathedral—a contribution to the preservation of cultural heritage. Doctoral thesis. 2013. https://doi.org/10.53846/goediss-4185. Accessed 4 Jan 2022.
57. Angeli M. Multiscale study of stone decay by salt crystallization in porous networks. Doctoral thesis. 2007. https://tel.archives-ouvertes.fr/tel-00239456. Accessed 21 Jan 2022.
58. Badawy A. Historical seismicity of Egypt. Acta Geod Geophys Hung. 1999;34(1–2):119–35. https://doi.org/10.1007/BF03325564.
59. Soliman MM. The Dahshour (Egypt) Earthquake of 12th of October 1992. October, 1992. International conferences on recent advances in geotechnical earthquake engineering and soil dynamics; 1995: 14. https://scholarsmine.mst.edu/icrageesd/03icrageesd/session07/14. Accessed 18 Jan 2022.
60. Mossaad M. Liquefaction during the october 12, 1992Dahshour, Egypt, earthquake and its potential in the Nile Valley and Delta. Soils Found. 1996;36(2):13–27. https://doi.org/10.3208/sandf.36.2_13.
61. Moustafa SSR, Takenaka H. Stochastic ground motion simulation of the 12 October 1992 Dahshour earthquake. Acta Geophys. 2009;57(3):636–56. https://doi.org/10.2478/s11600-009-0012-y.

62. Bares L. Foundation deposits in the tomb of Udjahorresnet at Abusir. Z Aegypt Sprach Altertumskd. 1996;123(1):1–9. https://doi.org/10.1524/zaes.1996.123.1.1.
63. Bureau of Indian Standards. Method of test for aggregate for concrete. IS 2386-Part III—Specific gravity, density, voids, absorption and bulking. 1963; New Delhi, (Reaffirmed 2002). https://law.resource.org/pub/in/bis/S03/is.2386.1.1963.pdf . Accessed 13 Mar 2022.
64. ASTM. C97/C97 M-18 Standard Test Methods for Absorption and Bulk Specific Gravity of Dimension Stone, ASTM International, West Conshohocken, PA. 2018. www.astm.org. Accessed 13 Mar 2022.
65. Standard test methods for laboratory determination of water (moisture) content of soil and rock by mass. www.astm.org, https://www.astm.org/d2216-19.html. Accessed 21 Jan 2022.
66. Pereira D. Stone testing. In: Pereira D, editor. Natural stone and world heritage. 1st ed. Boca Raton: CRC Press; 2019. p. 37–89. https://doi.org/10.1201/9781351013352-6.
67. Datta D, Thakur N, Ghosh S, Poddar R, Sengupta S. Determination of Porosity of Rock Samples from Photomicrographs Using Image Analysis. 2016 IEEE 6th International Conference on Advanced Computing (IACC). 2016. https://doi.org/10.1109/IACC.2016.67.
68. Siegesmund S, Snethlage R. Stone in Architecture. Berlin: Springer. 2011. https://link.springer.com/book/10.1007%2F978-3-642-14475-2 Accessed 8 Mar 2022.
69. Rafiei B, Rahmani S. Textural pattern of secondary gypsum in the basal anhydrite of the Asmari formation SW Iran. Geopersia. 2017;7(2):267–78. https://doi.org/10.22059/geope.2017.229055.648305.
70. Whitney DL, Evans BW. Abbreviations for names of rock-forming minerals. Am Mineral. 2009;95(1):185–7. https://doi.org/10.2138/am.2010.3371.
71. Mahrous AM, Tantawi MM, El-Sageer H. Evaluation of the engineering properties of some Egyptian limestones as construction materials for highway pavements. Constr Build Mater. 2010;24(12):2598–603. https://doi.org/10.1016/j.conbuildmat.2010.05.016.
72. Odom IE. Smectite clay minerals: properties and uses. Math Phys Eng Sci. 1984;311(1517):391–409. https://doi.org/10.1098/rsta.1984.0036.
73. McKinley JM, Worden RH, Ruffell AH. Smectite in sandstones: a review of the controls on occurrence and behaviour during diagenesis. Clay Miner Cem Sandstones. 1999. https://doi.org/10.1002/9781444304336.ch5.
74. Hemeda S, Fahmy A, Moustafa A, Hafez MAE. The early Basilica church, El-Ashmonein archaeological site, Minia, Egypt: geo-environmental analysis and engineering characterization of the building materials. Open J Geol. 2019;09(03):157–86. https://doi.org/10.4236/ojg.2019.93011.
75. Sparks DL. Inorganic soil components. Environ Soil Chem. 2003. https://doi.org/10.1016/B978-012656446-4/50002-5.
76. Tiennot M, Mertz J-D, Bourgès A. Influence of clay minerals nature on the hydromechanical and fracture behaviour of stones. Rock Mech Rock Eng. 2019;52(6):1599–611. https://doi.org/10.1007/s00603-018-1672-1.
77. Aldoasri M, Darwish S, Adam M, Elmarzugi N, Ahmed S. Enhancing the durability of calcareous stone monuments of ancient egypt using CaCO3 nanoparticles. Sustainability. 2017;9(8):1392. https://doi.org/10.3390/su9081392.
78. Kumar A. Industrial Pollution and Management. 1th ed. Delhi: APH publishing cooperation Google Books. APH Publishing; 2004. https://books.google.com/books?id=xk9SX3heeRkC&pgis=1. Accessed 08 Mar 2022.
79. Charola AE. Salts in the deterioration of porous materials: an overview. J Am Inst. 2000;39(3):327–43. https://doi.org/10.1179/019713600806113176.
80. Alves C, Figueiredo CAM, Sanjurjo-Sánchez J, Hernández AC. Salt weathering of natural stone: a review of comparative laboratory studies. Heritage. 2021;4(3):1554–65. https://doi.org/10.3390/heritage4030086.
81. Wang G, Li P, Hao F, Zou H, Yu X. Dolomitization process and its implications for porosity development in dolostones: a case study from the Lower Triassic Feixianguan Formation, Jiannan area, Eastern Sichuan Basin, China. J Pet Sci Eng. 2015;131:184–99. https://doi.org/10.1016/j.petrol.2015.04.011.
82. Turkington AV, Paradise TR. Sandstone weathering a century of research and innovation. Geomorphology. 2005;67(1–2):229–53. https://doi.org/10.1016/j.geomorph.2004.09.028.
83. Zhang Z, Liu J, Li B, Yang X. Thermally induced deterioration behaviour of two dolomitic marbles under heating–cooling cycles. R Soc Open Sci. 2018;5(10): 180779. https://doi.org/10.1098/rsos.180779.
84. Sweeny D. UCLA Encyclopedia of Egyptology. UCLA Encycl Egyptol. 2011. http://digital2.library.ucla.edu/viewItem.do?ark=21198/zz0027fc04. Accessed 9 Mar 2022.
85. Ahmed HT. Physical and mechanical characteristics of helwan limestone: for conservation treatment of ancient Egyptian limestone monuments. J Am Sci. 2015;11(2):136.
86. Sievert T, Wolter A, Singh NB. Hydration of anhydrite of gypsum (CaSO4.II) in a ball mill. Cem Concr Res. 2005;35(4):623–30. https://doi.org/10.1016/j.cemconres.2004.02.010.
87. Hong D, Fan M, Yu L. An experimental study simulating the dissolution of gypsum rock. Energy Explor Exploit. 2018;36(4):942–54. https://doi.org/10.1177/0144598717751927.
88. Kumral M, Abdelnasser A, Budakoglu M. Geochemistry of hydrothermal alteration associated with cenozoic intrusion-hosted Cu-Pb-Zn mineralization at tavşanlı area, Kütahya, NW Turkey. Minerals. 2016. https://doi.org/10.3390/min6010013.
89. Smith KL, Milnes AR, Eggleton RA. Weathering of basalt: formation of iddingsite. Clays Clay Miner. 1987;35(6):418–28. https://doi.org/10.1346/CCMN.1987.0350602.
90. Ünal M, Altunok E. Determination of water absorption properties of natural building stones and their relation to porosity. E J New World Sci Acad. 2019;14(1):39–45. https://doi.org/10.12739/nwsa.2019.14.1.1a0429.
91. Ozcelik Y, Ozguven A. Water absorption and drying features of different natural building stones. Constr Build Mater. 2014;63:257–70. https://doi.org/10.1016/j.conbuildmat.2014.04.030.
92. Li Z. Introduction to Concrete. Adv Concr Technol. 2011. https://doi.org/10.1002/9780470950067.ch1.

Publisher's Note